Optimizing Information Freshness using Low-Power Status Updates via Sleep-Wake Scheduling

Ahmed M. Bedewy
Department of ECE
The Ohio State University
Columbus, OH
bedewy.2@osu.edu

Yin Sun
Department of ECE
Auburn University
Auburn, AL
yzs0078@auburn.edu

Rahul Singh
Department of ECE
The Ohio State University
Columbus, OH
singh.1434@osu.edu

Ness B. Shroff
Departments of ECE and CSE
The Ohio State University
Columbus, OH
shroff.11@osu.edu

ABSTRACT

In this paper, we consider the problem of optimizing the freshness of status updates that are sent from a large number of low-power source nodes to a common access point. The source nodes utilize carrier sensing to reduce collisions and adopt an asychronized sleep-wake strategy to achieve an extended battery lifetime (e.g., 10-15 years). We use *age of information* (AoI) to measure the freshness of status updates, and design the sleep-wake parameters for minimizing the weighted-sum peak AoI of the sources, subject to per-source battery lifetime constraints. When the sensing time is zero, this sleep-wake design problem can be solved by resorting to a two-layer nested convex optimization procedure; however, for positive sensing times, the problem is non-convex. We devise a low-complexity solution to solve this problem and prove that, for practical sensing times that are short and positive, the solution is within a small gap from the optimum AoI performance. Our numerical and NS-3 simulation results show that our solution can indeed elongate the batteries lifetime of information sources, while providing a competitive AoI performance.

CCS CONCEPTS

• **Networks → Network performance evaluation**; *Network performance analysis*;

KEYWORDS

Age of information; Energy consumption; Sleep-wake; Multi-source

ACM Reference Format:
Ahmed M. Bedewy, Yin Sun, Rahul Singh, and Ness B. Shroff. 2020. Optimizing Information Freshness using Low-Power Status Updates via Sleep-Wake Scheduling. In *The Twenty-first ACM International Symposium on Theory, Algorithmic Foundations, and Protocol Design for Mobile Networks and Mobile Computing (Mobihoc '20), October 11–14, 2020, Boston, MA, USA.* ACM, Online,, 10 pages. https://doi.org/10.1145/3397166.3409125

Mobihoc '20, October 11–14, 2020, Boston, MA, USA

ACM ISBN 978-1-4503-8015-7/20/10…$15.00
https://doi.org/10.1145/3397166.3409125

1 INTRODUCTION

In applications such as networked monitoring and control systems, wireless sensor networks, autonomous vehicles, it is crucial for the destination node to receive timely status updates so that it can make accurate decisions. *Age of information* (AoI) has been used to measure the freshness of status updates. More specifically, AoI [20] is the age of the freshest update at the destination, i.e., it is the time elapsed since the most recently received update was generated. It must be noted that optimizing traditional network performance metrics such as throughput or delay do not attain the goal of timely updating. For instance, it is well known that AoI could become very large when the offered load is high or low [20]. As a result, AoI has recently attracted a lot of interests (see [30] and references therein).

In a variety of information update systems, energy consumption is also a critical constraint. For example, wireless sensor networks are used for monitoring crucial natural and human-related activities, e.g. forest fires, earthquakes, tsunamis, etc. Since such applications often require the deployment of sensor nodes in remote or hard-to-reach areas, they need to be able to operate unattended for long durations. Likewise, in medical sensor networks, since battery replacement/recharging involves a series of medical procedures, thereby providing disutility to patients, energy consumption must be constrained in order to support a long battery life of up to 10-15 years [35]. Therefore, for networks serving such real-time applications, prolonging battery-life is just as crucial as guaranteeing a small AoI. Existing works on multi-source networks, e.g., [12, 13, 15, 17–19, 23, 33, 34, 39], focused exclusively on minimizing the AoI and overlooked the need to reduce power consumption. This motivates us to derive algorithms that achieve a trade-off between the competing tasks of minimizing AoI and reducing the energy consumption in multi-source networks.

Additionally, some applications are characterized by a large number (typically hundreds of thousands) of densely packed wireless nodes serviced by only a single access point (AP). Examples include machine-type communication [21]. The dataloads in such "dense

networks" [21, 22] are created by applications such as home security and automation, oilfield and pipeline monitoring, smart agriculture, animal tracking and livestock, etc. This introduces high variability in the data packet sizes so that the transmission times of data packets are random. Thus scheduling algorithms that are designed for time-slotted systems with a fixed transmission duration, are not applicable to these systems. Besides that, synchronized scheduler for time-slotted systems are feasible when there are relatively few sources and each source has sufficient energy. However, if there are a huge number of sources, and each source has limited energy and low traffic rate, coordinating synchronized transmissions is quite challenging. This motivates us to design randomized protocols that coordinate the transmissions of multiple conflicting transmitters connected to a single AP.

Towards that end, we consider a wireless network with M sources that contend for channel access and communicate their update packets to an AP. Each source is equipped with a battery that may get charged by a renewable source of energy, e.g., solar. Moreover, each source employs a "sleep-wake" scheme [9] under which it transmits a packet if the channel is sensed idle; and sleeps if either: (i) It senses the channel to be busy, (ii) it completes a packet transmission. This enables each source to save the precious battery power by switching off at times when it is unlikely to gain channel access for packet transmissions.

However, since a source cannot transmit during the sleep period, this causes the AoI to increase. We thus carefully design these sleeping periods so that the cumulative weighted average peak age of all sources is minimized, while ensuring that the energy consumption of each source is below its average battery power.

1.1 Related Works

There has been a significant effort on analyzing the AoI performance of popular queueing service disciplines, e.g., the First-Come, First-Served (FCFS) [20] Last-Come, First-Served (LCFS) with and without preemption [40], and queueing systems with packet management [10]. In [3–6, 31], the age-optimality of Last-Generated, First-Served (LGFS)-type policies in multi-server and multi-hop networks was established, where it was shown that these policies can minimize any non-decreasing functional of the age processes. The fundamental coupling of data sampling and transmission in information update systems was investigated in [29, 32], where sampling policies were designed to minimize any nonlinear age function in single source systems. In particular, [29] shows that, under certain conditions, monotonic functions of the age can represent auto-correlation functions, estimation error, mutual information, and conditional entropy. The studies in [29, 32] were later extended to a multi-source scenario in [1, 2].

Designing scheduling policies for minimizing AoI in multi-source networks has recently received increasing attention, e.g., [12, 13, 15, 17–19, 23, 33, 34, 39]. Of particular interest, are those pertaining to designing distributed scheduling policies [15, 17, 19, 23, 33, 39]. The work in [39] considered slotted ALOHA-like random access scheme in which each node accesses the channel with a certain access probability. These probabilities were then optimized in order to minimize the AoI. However, the model of [39] allows multiple interfering users to gain channel access simultaneously, and hence allows for the collision. The authors in [33] generalized the work in [39] to a wireless network in which the interference is described by a general interference model. The Round Robin or Maximum Age First policy was shown to be (near) age-optimal for different system models, e.g., in [15, 17, 19, 23].

A central component of the scheme proposed in this work is the carrier sensing mechanism in which sources sense the channel to detect times during which no interfering transmissions occur. We note that such mechanisms are employed in numerous distributed medium-access schemes in wireless networks, such as Carrier Sense Multiple Access (CSMA), see [41] for a recent survey of the existing schemes. Thus, there has been an interest in designing CSMA-based scheduling schemes that optimize the AoI [25, 38]. In [25], the authors employed the standard idealized CSMA in [16] to minimize the AoI with an exponentially distributed packet transmission times. In [38], the authors employed the slotted Carrier Sense Multiple Access/Collision-Avoidance (CSMA/CA) in [8] to minimize the broadcast age of information, which is defined, from a sender perspective, as the age of the freshest successfully broadcasted packet. Contrary to these works, the sleep-wake scheme proposed by us emphasizes on reducing the cumulative energy consumption in multi-source networks in addition to minimizing the cumulative weighted AoI. Moreover, in our study, transmission times are not necessarily random variables with some commonly used parametric density [25], or deterministic [38], but can be any generally distributed random variables with finite mean.

1.2 Key Contributions

Our key contributions are summarized as follows:

- The problem of minimizing the total weighted average peak age over the sources, while simultaneously meeting per-source energy constraints is non-convex. Nonetheless, we devise a solution, i.e., a choice of the mean sleeping durations for each source. We then show that in the regime for which the sensing time is negligible compared to the packet transmission time, the proposed solution is near-optimal (Theorem 3.1 and Theorem 3.3). Our near-optimality results hold for any generally distributed packet transmission times.
- We propose an algorithm that can be easily implemented in many industrial control systems. In particular, we are able to represent our solution in a form that requires the knowledge of two variables to obtain its value. These two variables are functions of the network parameters, i.e., the mean packet transmission times, the carrier sensing time, the number of source nodes, the battery size and the importance weight of each source. A communication procedure to collect these two variables from each source node is provided. Because only two variables are needed, the communication overhead is quite low.
- Finally, in the limiting scenario, when the ratio between the sensing time and the packet transmission time goes to zero, we show that the age performance of our proposed algorithm is as good as that of the optimal synchronized scheduler (e.g., for time-slotted systems), in which the time overhead needed for coordinating different sources with random packet sizes are omitted (Corollary 3.5). Hence, this comes with an extra

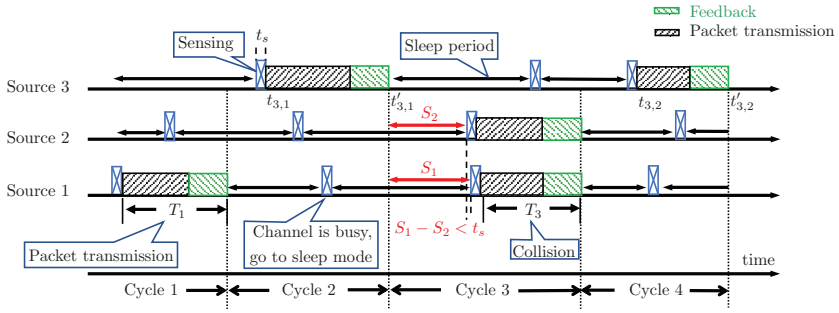

Figure 1: Illustration of the sleep-wake cycles. In Cycle 1-2, we have successful packet transmissions. Let S_1 and S_2 represent the remaining sleeping times of Sources 1 and 2, respectively, after a successful transmission. Then, a collision occurs in Cycle 3 because the difference between wake-up times of Sources 1 and 2 is less than t_s, i.e., $S_1 - S_2 < t_s$. As we can observe, each cycle consists of an idle period before a transmission/collision event.

advantage towards our algorithm of having less signaling overhead.

2 MODEL AND FORMULATION

2.1 Network Model and Sleep-wake Scheduling

Consider a wireless network composed of M source nodes observing time-varying processes. Sources generate update packets and communicate them to an access point (AP) over the same spectrum band. If multiple sources transmit packets simultaneously, a packet collision occurs and the corresponding packet transmissions fail.

We assume that the sources use a sleep-wake scheduling scheme to access the shared channel, where the sources switch between a sleep mode and transmission mode over time, according the following rules: Upon waking from the sleep mode, a source first performs carrier sensing to check whether the channel is occupied by another source, as illustrated in Figure 1. We assume that the sources are within the hearing range of each other. The time duration of carrier sensing is denoted as t_s, which is sufficiently long to ensure a high sensing accuracy. If the channel is sensed to be busy, the source enters the sleep mode directly; otherwise, the source generates and transmits an update packet over the channel. Upon completing a packet transmission, the source goes back to the sleep mode.

In the above sleep-wake scheduling scheme, if two sources start transmitting within a duration of t_s, then they may not be able to sense the transmission of each other. In order to obtain a robust system design, we consider that they cannot detect each other's transmission in this case and a collision occurs. A feedback is sent back to the sources to indicate the outcome of their transmissions (successful transmission or collision).

A *sleep-wake* cycle, or simply a *cycle*, is defined as the time period between the ends of two successive packet transmission or collision events in the network. Each cycle consists of an idle period and a transmission/collision duration[1]. As depicted in Figure 1, the packet transmissions in Cycle 1-2 are successful, but a collision occurs in Cycle 3 because Sources 1 and 2 wake up within a short duration t_s.

We use $T_i, i \in \{1, 2, \ldots\}$ to represent the time incurred during the i-th packet transmission or collision event over time, which includes propagation and feedback delays. For example, in Figure 1, T_1 is the duration of the packet transmission event by Source 1, while T_3 is the duration of the collision event between Source 1 and 2. We assume that the distribution of the time spent during transmission or collision is the same. In Section 5.1, we show that this assumption has a negligible impact on the performance of the proposed algorithm. The transmission/collision times T_i's are i.i.d. across time and sources, and are generally distributed. In the rest of the paper, we omit the subscript i of T_i for simplicity, and use T to denote the transmission/collision time, which is assumed to have a finite mean, i.e., $E[T] < \infty$. The sleep periods of source l are exponentially distributed random variables with mean value $\mathbb{E}[T]/r_l$ and are independent across sources and *i.i.d.* across time. Here, the sleep period parameter r_l has been normalized by the mean transmission time $\mathbb{E}[T]$. Let $\mathbf{r} = (r_1, \ldots, r_M)$ be the vector comprising of these sleep period parameters.

2.2 Total Weighted Average Peak Age

Let α_l be the probability of the event that the source l obtains channel access and successfully transmits a packet within a cycle. As shown in [9], one can utilize the property of exponential distributed sleep periods to get that

$$\alpha_l = \frac{r_l e^{r_l \frac{t_s}{\mathbb{E}[T]}}}{e^{\sum_{i=1}^{M} r_i \frac{t_s}{\mathbb{E}[T]}} \sum_{i=1}^{M} r_i}. \tag{1}$$

For the sake of completeness, we derive the above expression in our technical report [7, Appendix A]. Let N_l denote the total number of cycles between two successful transmissions of source l. Now, if the probability that source l obtains channel access and transmits successfully in a given cycle is α_l, and $1 - \alpha_l$ otherwise, then N_l is geometrically distributed with mean $\frac{1}{\alpha_l}$. Thus, we get

$$\mathbb{E}[N_l] = \frac{e^{\sum_{i=1}^{M} r_i \frac{t_s}{\mathbb{E}[T]}} \sum_{i=1}^{M} r_i}{r_l e^{r_l \frac{t_s}{\mathbb{E}[T]}}}. \tag{2}$$

[1]To make the sleep-wake scheduling problem solvable analytically, we make several approximations. For example, we suppose that each cycle must start with an idle period where all sources are in the sleep mode and omit all events that violate this structure. NS-3 simulation results will be provided in Section 5.1 to show that these approximations have a negligible impact on the age performance of our solution.

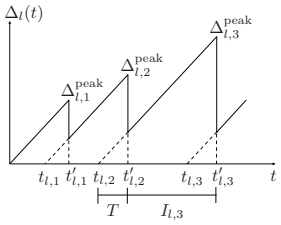

Figure 2: The age evolution of source l ($\Delta_l(t)$).

Let $U_l(t)$ represent the generation time of the most recently delivered packet from source l by time t. Then, the *age of information*, or simply the *age*, of source l is defined as [20]

$$\Delta_l(t) = t - U_l(t), \tag{3}$$

where $\Delta_l(t)$ is right-continuous. Since a fresh packet is delivered each time a source obtains channel access and completes transmission, the AoI of source l is reset to the transmission time of the delivered packet after a random number of N_l cycles.

We begin by introducing some notations and definitions. We use $t_{l,i}$ and $t'_{l,i}$ to denote the generation and delivery times, respectively, of the i-th delivered packet from source l, where we have $t'_{l,i} - t_{l,i} = T$.[2] Let $I_{l,i} = t'_{l,i} - t'_{l,i-1}$ denote the i-th inter-departure time of source l, where we have $\mathbb{E}[I_{l,i}] = \mathbb{E}[I_l] \leq \infty$ for all i. The i-th peak age of source l, denoted by $\Delta_{l,i}^{\text{peak}}$, is defined as the AoI of source l right before the i-th packet delivery from source l, as shown in Figure 2, i.e., we have

$$\Delta_{l,i}^{\text{peak}} = \Delta_l(t'^{-}_{l,i}), \tag{4}$$

where $t'^{-}_{l,i}$ is the time instant just before the delivery time $t'_{l,i}$. One can observe from Figure 2 that the peak age is [10]

$$\Delta_{l,i}^{\text{peak}} = I_{l,i} + T. \tag{5}$$

Hence, the average peak age of source l is given by

$$\mathbb{E}[\Delta_{l,i}^{\text{peak}}] = \mathbb{E}[I_l] + \mathbb{E}[T]. \tag{6}$$

We now derive an expression for $\mathbb{E}[I_l]$. An inter-departure time duration of a particular source is composed of multiple consecutive sleep-wake cycles, see Figure 1. With a slight abuse of notation, we let $\mathbf{cycle}_{l,i}$ denote the duration of the i-th sleep-wake cycle after a successful transmission of source l. Hence, we have

$$\mathbb{E}[I_l] = \mathbb{E}\left[\sum_{i=1}^{N_l} \mathbf{cycle}_{l,i}\right]. \tag{7}$$

Note that $\mathbf{cycle}_{l,i}$'s are i.i.d. across time. Moreover, since $\mathbb{P}(N_l = n)$ depends only on the history, N_l is a stopping time [28]. Hence, it follows from Wald's identity [37] that

$$\mathbb{E}[I_l] = \mathbb{E}[N_l]\mathbb{E}[\mathbf{cycle}], \tag{8}$$

where $\mathbb{E}[\mathbf{cycle}]$ is the mean duration of a sleep-wake cycle. Each cycle consists of an idle period and a transmission/collision time, see Figure 1. Using the memoryless property of exponential distribution, we observe that the idle period is the minimum of exponential random variables. Thus, it can be shown that the idle period in each cycle is exponentially distributed with mean value equal to $\mathbb{E}[T]/\sum_{i=1}^{M} r_i$, where $\mathbb{E}[T]/r_l$ is the mean of sleep periods of source l. Hence, we have

$$\mathbb{E}[\mathbf{cycle}] = \frac{\mathbb{E}[T]}{\sum_{i=1}^{M} r_i} + \mathbb{E}[T]. \tag{9}$$

Substituting the expressions for $\mathbb{E}[N_l]$ and $\mathbb{E}[\mathbf{cycle}]$ from (2) and (9), respectively, into (8), and then into (6), we obtain

$$\mathbb{E}[\Delta_{l,i}^{\text{peak}}] = \frac{e^{-r_l \frac{t_s}{\mathbb{E}[T]}}\mathbb{E}[T]}{r_l} e^{\sum_{i=1}^{M} r_i \frac{t_s}{\mathbb{E}[T]}} \left(1 + \sum_{i=1}^{M} r_i\right) + \mathbb{E}[T]. \tag{10}$$

In this paper, we aim to minimize the total weighted average peak age, which is given by

$$\sum_{l=1}^{M} \frac{w_l e^{-r_l \frac{t_s}{\mathbb{E}[T]}}\mathbb{E}[T]}{r_l} e^{\sum_{i=1}^{M} r_i \frac{t_s}{\mathbb{E}[T]}} \left(1 + \sum_{i=1}^{M} r_i\right) + \sum_{l=1}^{M} w_l \mathbb{E}[T], \tag{11}$$

where $w_l > 0$ is the weight of source l. These weights enable us to prioritize the sources according to their relative importance [33, 34].

2.3 Energy Constraint

Each source is equipped with a battery that can possibly be recharged by a renewable energy source, such as solar. The energy constraint on source l is described by the following parameters: a) Initial battery level B_l, which denotes the initial amount of energy stored in its battery, b) Target lifetime D_l, which is the minimum time-duration that the source l should be active before its battery is depleted, c) Average energy replenishment rate[3] R_l, which is the rate at which the battery of source l receives energy from its energy source. Observe that if source l does not have access to an energy source, then we have $R_l = 0$.

In typical wireless sensor networks, sources have a much smaller power consumption in the sleep mode than in the transmission mode. For example, if the sensor is equipped with the radio unit TR 1000 from RF Monolithic [27, 36], the power consumption in the sleep mode is 15 μW while the power consumption in the transmission mode is 24.75 mW. Motivated by this, we assume that the energy dissipation during the sleep mode is negligible as compared to the power consumption in the transmission mode. Moreover, we assume that the sensing time duration t_s is very short as compared to the transmission time and hence neglect the energy consumed while sensing the channel. In Section 5.1, we show that these assumptions have a negligible effect on the performance of the proposed algorithm. Under these assumptions, the amount of energy used by a source is equal to the amount of energy consumed in transmissions. Note that the power consumed in packet transmission is equal to the sum of energy consumed while using radio signal during packet transmission, and the power used for receiving feedback.

The maximum allowable energy consumption rate for transmissions, denoted by $E_{\text{con},l}$, is given by

$$E_{\text{con},l} = \frac{B_l}{D_l} + R_l, \ \forall l. \tag{12}$$

[2] A packet of a particular source is deemed delivered when the source receives the feedback.

[3] It is assumed that R_l is either known, or it can be estimated accurately.

Then, for source l to achieve its target lifetime, D_l, the actual energy consumption rate of source l, E_l, must satisfy

$$E_l \leq E_{\text{con},l}, \ \forall l. \tag{13}$$

For the sleep-wake mechanism under consideration, it has been shown in [9] that the total fraction of time in which source l transmits update packets is given by

$$\sigma_l = \frac{[1 - e^{-r_l \frac{t_s}{\mathbb{E}[T]}}] \sum_{i=1}^{M} r_i + r_l e^{-r_l \frac{t_s}{\mathbb{E}[T]}}}{\sum_{i=1}^{M} r_i + 1}. \tag{14}$$

For the sake of completeness, the derivation of σ_l is discussed in our technical report [7, Appendix B]. If $E_{\text{avg},l}$ is the average energy consumption rate of source l in the transmission mode, then we have

$$E_l = \sigma_l E_{\text{avg},l}, \ \forall l. \tag{15}$$

Define $b_l \triangleq E_{\text{con},l}/E_{\text{avg},l}$ as the target energy efficiency of source l. Then, the energy constraints in (13) can be rewritten as

$$\sigma_l = \frac{[1 - e^{-r_l \frac{t_s}{\mathbb{E}[T]}}] \sum_{i=1}^{M} r_i + r_l e^{-r_l \frac{t_s}{\mathbb{E}[T]}}}{\sum_{i=1}^{M} r_i + 1} \leq b_l, \ \forall l. \tag{16}$$

Observe that if $b_l \geq 1$, then constraint (16) is always satisfied.

2.4 Problem Formulation

Our goal is to design $\mathbf{r}$ in order to minimize the total weighted average peak age in (11), while simultaneously ensuring that the energy constraints (16) are satisfied. After normalizing the total weighted average peak age in (11) by $\mathbb{E}[T]$, our goal can be cast as the following optimization problem: (Problem **1**)

$$\begin{aligned} \bar{\Delta}_{\text{opt}}^{\text{w-peak}} \triangleq \min_{r_l>0} & \sum_{l=1}^{M} \frac{w_l e^{-r_l \frac{t_s}{\mathbb{E}[T]}}}{r_l} e^{\sum_{i=1}^{M} r_i \frac{t_s}{\mathbb{E}[T]}} \left(1 + \sum_{i=1}^{M} r_i\right) + \sum_{l=1}^{M} w_l \\ \textbf{s.t.} \ & \frac{[1 - e^{-r_l \frac{t_s}{\mathbb{E}[T]}}] \sum_{i=1}^{M} r_i + r_l e^{-r_l \frac{t_s}{\mathbb{E}[T]}}}{\sum_{i=1}^{M} r_i + 1} \leq b_l, \forall l, \end{aligned} \tag{17}$$

where $\bar{\Delta}_{\text{opt}}^{\text{w-peak}}$ is the optimal objective value of Problem **1**. We will use $\bar{\Delta}^{\text{w-peak}}(\mathbf{r})$ to denote the objective function of Problem **1** for given sleeping period parameters $\mathbf{r}$. One can notice from (17) that the optimal sleeping period parameters depends on the sensing time t_s and the mean transmission time $\mathbb{E}[T]$ only through their ratio $t_s/\mathbb{E}[T]$. This insight plays a crucial role in subsequent analysis of Problem **1**.

3 MAIN RESULTS

We can observe that Problem **1** can be solved by resorting to nested convex optimization, if the sensing time is zero. Although Problem **1** is non-convex even when $t_s/\mathbb{E}(T) = 0$, it can be solved by defining an auxiliary variable $y = \sum_{i=1}^{M} r_i + 1$ and applying a nested optimization algorithm: In the inner layer, we optimize r_l for a given y. Then, we write the optimized objective as a function of y. In the outer layer, we optimize y. It happens that the inner and outer layer optimization problems are both convex. More detail is followed in Section 3.3.

However, this method does not work for positive sensing times and Problem **1** becomes non-convex. Hence, it is challenging to solve for optimal $\mathbf{r}$. In this section we will propose a low-complexity closed-form solution which is near-optimal when the sensing time is small as compared with the transmission time. Our solution is developed by considering the following two regimes separately: (i) *Energy-adequate regime* denoted as $\sum_{i=1}^{M} b_i \geq 1$, where the condition $\sum_{i=1}^{M} b_i \geq 1$ means that the sources have a sufficient amount of total energy to ensure that at least one source is awake at any time, (ii) *Energy-scarce regime* represented by $\sum_{i=1}^{M} b_i < 1$, which indicates that the sources have to sleep for some time to meet the sources' energy constraints.

3.1 Energy-adequate Regime

In the energy-adequate regime $\sum_{i=1}^{M} b_i \geq 1$, our solution $\mathbf{r}^\star := (r_1^\star, \ldots, r_M^\star)$ is given as

$$r_l^\star = \min\{b_l, \beta^\star \sqrt{w_l}\} x^\star, \forall l, \tag{18}$$

where $x^\star$ and $\beta^\star$ are expressed in terms of the the parameters $\{b_i, w_i\}_{i=1}^{M}, t_s/\mathbb{E}[T]$ as follows:

$$x^\star = \frac{-1}{2} + \sqrt{\frac{1}{4} + \frac{\mathbb{E}[T]}{t_s}}, \tag{19}$$

and $\beta^\star$ is the root of

$$\sum_{i=1}^{M} \min\{b_i, \beta^\star \sqrt{w_i}\} \ = 1. \tag{20}$$

The performance of the above solution $\mathbf{r}^\star$ is manifested in the following theorem:

Theorem 3.1 (**Near-optimality**). *If $\sum_{i=1}^{M} b_i \geq 1$, then the solution $\mathbf{r}^\star$ given by* (18) - (20) *is near-optimal for solving* (17) *when $t_s/E[T]$ is sufficiently small, in the following sense:*[4]

$$\left| \bar{\Delta}^{w\text{-}peak}(\mathbf{r}^\star) - \bar{\Delta}_{opt}^{w\text{-}peak} \right| \leq 2\sqrt{\frac{t_s}{\mathbb{E}[T]}} C_1 + o\left(\sqrt{\frac{t_s}{\mathbb{E}[T]}}\right), \tag{21}$$

where

$$C_1 = \sum_{i=1}^{M} \frac{w_i}{\min\{b_i, \beta^\star \sqrt{w_i}\}}. \tag{22}$$

Proof. See Section 4. □

As a result of Theorem 3.1, we can obtain the following corollary:

Corollary 3.2 (**Asymptotic optimality**). *If $\sum_{i=1}^{M} b_i \geq 1$, then the solution $\mathbf{r}^\star$ given by* (18) - (20) *is asymptotically optimal for the Problem **1** as $t_s/\mathbb{E}[T] \to 0$, i.e.,*

$$\lim_{\frac{t_s}{\mathbb{E}[T]} \to 0} \left| \bar{\Delta}^{w\text{-}peak}(\mathbf{r}^\star) - \bar{\Delta}_{opt}^{w\text{-}peak} \right| = 0. \tag{23}$$

*Moreover, the asymptotic optimal value of Problem **1** as $t_s/\mathbb{E}[T] \to 0$ is*

$$\lim_{\frac{t_s}{\mathbb{E}[T]} \to 0} \bar{\Delta}_{opt}^{w\text{-}peak} = \sum_{i=1}^{M} \left[\frac{w_i}{\min\{b_i, \beta^\star \sqrt{w_i}\}} + w_i \right]. \tag{24}$$

Proof. See Section 4. □

[4] We use the standard order notation: $f(h) = O(g(h))$ means $z_1 \leq \lim_{h \to 0} f(h)/g(h) \leq z_2$ for some constants $z_1 > 0$ and $z_2 > 0$, while $f(h) = o(g(h))$ means $\lim_{h \to 0} f(h)/g(h) = 0$.

3.2 Energy-scarce Regime

Now, we present a solution to Problem **1** and show it is near-optimal in energy-scarce regime $\sum_{i=1}^{M} b_i < 1$. The solution $\mathbf{r}^\star$ of the energy-scarce regime is again given by (18), where $x^\star$ and $\beta^\star$ are

$$x^\star = \frac{\min_l c_l}{1-\sum_{i=1}^{M} b_i},\ \beta^\star = \sum_{i=1}^{M} \frac{1}{\sqrt{w_i}}, \tag{25}$$

and

$$c_l = \frac{2b_l\left(1-\sum_{i=1}^{M} b_i\right)^2}{Q}, \tag{26}$$

$$Q = b_l\left(1-\sum_{i=1}^{M} b_i\right)^2 + \sqrt{b_l^2\left(1-\sum_{i=1}^{M} b_i\right)^4 + 4b_l^2\left(1-\sum_{i=1}^{M} b_i\right)^2\left(\sum_{i=1}^{M} b_i - b_l\right)\frac{t_s}{\mathbb{E}[T]}}. \tag{27}$$

The near-optimality of the proposed solution (i.e., $\mathbf{r}^\star$) in the energy scarce regime is explained in the following theorem:

Theorem 3.3 (**Near-optimality**). *If $\sum_{i=1}^{M} b_i < 1$, then the solution $\mathbf{r}^\star$ given by* (18) *and* (25) - (27) *is near-optimal for solving* (17) *when $t_s/\mathbb{E}[T]$ is sufficiently small, in the following sense:*

$$\left|\bar{\Delta}^{w\text{-}peak}(\mathbf{r}^\star) - \bar{\Delta}_{opt}^{w\text{-}peak}\right| \le \frac{t_s}{\mathbb{E}[T]}C_2 + o\left(\frac{t_s}{\mathbb{E}[T]}\right), \tag{28}$$

where

$$C_2 = \sum_{l=1}^{M} \frac{w_l}{b_l(1-\sum_{i=1}^{M} b_i)}\left(3\sum_{i=1}^{M} b_i - \min_j b_j\right). \tag{29}$$

Proof. See our technical report [7]. □

From Theorem 3.3, we obtain the following corollary:

Corollary 3.4 (**Asymptotic optimality**). *If $\sum_{i=1}^{M} b_i < 1$, then* (23) *holds for the solution $\mathbf{r}^\star$ given by* (18) *and* (25) - (27). *In other words, our proposed solution is asymptotically optimal for the Problem **1** as $t_s/\mathbb{E}[T] \to 0$. Moreover, the asymptotic optimal value of Problem **1** as $t_s/\mathbb{E}[T] \to 0$ is*

$$\lim_{\frac{t_s}{\mathbb{E}[T]}\to 0} \bar{\Delta}_{opt}^{w\text{-}peak} = \sum_{i=1}^{M}\left[\frac{w_i}{\min\{b_i, \beta^\star\sqrt{w_i}\}} + w_i\right] = \sum_{i=1}^{M}\left[\frac{w_i}{b_i} + w_i\right]. \tag{30}$$

Proof. See our technical report [7]. □

Interestingly, the asymptotic optimal values of Problem **1** in both regimes, given by (24) and (30), are identical. However, in the energy-scarce regime, we can observe that $\beta^\star$, which is defined in (25), always satisfies $\min\{b_l, \beta^\star\sqrt{w_l}\} = b_l$ for all l.

Remark 1. We would like to point out that the condition $t_s/\mathbb{E}[T] \approx 0$ is satisfied in many practical applications. For instance, in a wireless sensor network that is equipped with low-power UHF transceivers [11], the carrier sensing time is $t_s = 40\ \mu$s, while the transmission time is around 5 ms. Hence, $t_s/\mathbb{E}[T] \approx 0.008$.

3.3 Discussion

In this subsection, we: (i) discuss a simple implementation of our proposed solution, (ii) discuss the nested convex optimization method that can be used to solve Problem **1** when $t_s = 0$, and (iii) provide some useful insights about our proposed solution at the limit point $t_s/\mathbb{E}[T] \to 0$. Due to space limitation, we move the second point to our technical report [7, Section 3.3.2].

3.3.1 Implementation of Sleep-wake Scheduling. We devise a simple algorithm to compute our solution $\mathbf{r}^\star$, which is provided in Algorithm 1. Notice that $\mathbf{r}^\star$ has the same expression (18) in the energy-adequate and energy-scarce regimes. We exploit this fact to simplify the implementation of sleep-wake scheduling. In particular, the sources report w_l and b_l to the AP, which computes $\beta^\star$ and $x^\star$, and broadcasts them back to the sources. After receiving $\beta^\star$ and $x^\star$, source l computes $r_l^\star$ based on (18). In practical wireless sensor networks, e.g., smart city networks and industrial control sensor networks [14, 24], the sensors report their measurements via an access point (AP). Hence, it is reasonable to employ the AP in implementing the sleep-wake scheduler.

Algorithm 1: Implementation of sleep-wake scheduler.

```
The AP gathers the parameters {(w_i, b_i)_{i=1}^M, t_s/E[T]};
if Σ_{i=1}^M b_i ≥ 1 then
    The AP derives x*, β* according to (19) and (20);
else
    The AP derives x*, β* according to (25) - (27);
end
The AP broadcasts x*, β* to all the M sources;
Upon hearing x*, β*, source l compute r_l* from (18);
```

In the above implementation procedure, the sources do need not know if the overall network is in the energy-adequate or energy-scarce regime; only the AP knows about it. Further, the amount of downlink signaling overhead is small, because only two parameters $\beta^\star$ and $x^\star$ are broadcasted to the sources. Moreover, when the node density is high, the scalability of the network is a crucial concern and reporting w_l and b_l for each source is impractical. In this case, the AP can compute $\beta^\star$ and $x^\star$ by estimating the distribution of w_l and b_l, as well as the number of source nodes, which reduces the uplink signaling overhead. Finally, when sources are not in the hearing range of each other, hidden/exposed source problems arise. These problems are challenging to solve analytically. However, this can be solved by designing practical heuristic solutions based on the theoretical solutions. See [9] as an example of this design method.

3.3.2 Asymptotic Behavior of The Optimal Solution. We would like to show that the performance of our proposed algorithm is asymptotically no worse than any synchronized scheduler (e.g., for time-slotted systems) in theory, for which we assume that the time overhead needed for coordinating different sources with random packet sizes are omitted. Note that because of the coordination overhead, such synchronized schedulers are only feasible when the number of sources M is small.

In synchronized schedulers, the AP assigns channel access among the sources in an i.i.d. manner. Under such a scheduler, there is a probability vector $\mathbf{a} = \{a_l\}_{l=1}^M$, $\sum_{i=1}^M a_i \le 1$, such that each source l gains channel access after a packet transmission with a probability

equal to a_l. Only one source is allowed to access the channel at a time (i.e., there is no collision)[5]. We can perform an analysis similar to that of Section 2.2, and show that the total weighted average peak age of a synchronized scheduler is given by

$$\sum_{i=1}^{M}\left[\frac{w_i\mathbb{E}[T]}{a_i}+w_i\,\mathbb{E}[T]\right]. \tag{31}$$

Moreover, similar to the derivation in our technical report [7, Appendix B], we can show that the fraction of time during which source l transmits update packets under a synchronized scheduler is equal to a_l. Hence, the problem of designing an optimal synchronized scheduler that minimizes the total weighted average peak age under energy constraints can be cast as

$$\bar{\Delta}^{\text{w-peak}}_{\text{opt-s}} \triangleq \min_{a_i>0}\sum_{i=1}^{M}\left[\frac{w_i}{a_i}+w_i\right] \tag{32}$$

$$\textbf{s.t. } a_l \le b_l,\ \forall l, \tag{33}$$

$$\sum_{i=1}^{M} a_i \le 1, \tag{34}$$

where we note that we have normalized the objective function by $\mathbb{E}[T]$. Next, we show that the performance of our proposed algorithm converges to that of the optimal synchronized scheduler when $t_s/\mathbb{E}[T]\to 0$.

Corollary 3.5. *For any $(w_i,b_i)_{i=1}^M$, we have*

$$\lim_{\frac{t_s}{\mathbb{E}[T]}\to 0}\bar{\Delta}^{w\text{-}peak}_{opt}=\bar{\Delta}^{w\text{-}peak}_{opt\text{-}s}. \tag{35}$$

Proof. See our technical report [7]. □

Synchronized schedulers were recently studied in [34] for the case without energy constraints, i.e., $b_l\ge 1$ for all l. According to Corollary 3.5, the channel access probability of the synchronized scheduler in [34] can be obtained from our solution.

4 PROOFS OF THE MAIN RESULTS

In this section, we provide the proofs of Theorem 3.1 and Corollary 3.2. The proofs of Theorem 3.3 and Corollary 3.4 have the same idea, and are provided in our technical report [7]. We prove Theorem 3.1 and Corollary 3.2 in three steps:

Step 1: We begin by showing that our solution $\mathbf{r}^\star$ given by (18) - (20) is feasible for Problem **1**.

Lemma 4.1. *If $\sum_{i=1}^M b_i\ge 1$, then the solution $\mathbf{r}^\star$ given by* (18) - (20) *is feasible for Problem **1**.*

Proof. See our technical report [7]. □

Hence, by substituting this solution $\mathbf{r}^\star$ into the objective function of Problem **1** in (17), we get an upper bound on the optimal value $\bar{\Delta}^{\text{w-peak}}_{\text{opt}}$, which is expressed in the following lemma:

[5]Note that if $\sum_{i=1}^M a_i<1$, then there is a probability that the scheduler decides not to serve any source. In this case, the scheduler waits for a random time that has the same distribution as the transmission time T before drawing the probability vector $\mathbf{a}$ again.

Lemma 4.2. *If $\sum_{i=1}^M b_i\ge 1$, then*

$$\bar{\Delta}^{w\text{-}peak}_{opt}\le\bar{\Delta}^{w\text{-}peak}(\mathbf{r}^\star)\le\sum_{i=1}^{M}\left[\frac{w_i e^{x^\star\frac{t_s}{\mathbb{E}[T]}}\left(1+\frac{1}{x^\star}\right)}{\min\{b_i,\beta^\star\sqrt{w_i}\}}+w_i\right], \tag{36}$$

where $x^\star$, $\beta^\star$ are defined in (19), (20).

Proof. See our technical report [7]. □

Step 2: We now construct a lower bound on the optimal value of Problem **1**. Suppose that $\mathbf{r}=(r_1,\ldots,r_M)$ is a feasible solution to Problem **1**, such that $r_l>0$ and

$$\frac{[1-e^{-r_l\frac{t_s}{\mathbb{E}[T]}}]\sum_{i=1}^M r_i+r_l e^{-r_l\frac{t_s}{\mathbb{E}[T]}}}{\sum_{i=1}^M r_i+1}\le b_l,\forall l. \tag{37}$$

Because $[1-e^{-r_l(t_s/\mathbb{E}[T])}]\sum_{i=1}^M r_i+r_l e^{-r_l(t_s/\mathbb{E}[T])}>r_l$ for all l, $\mathbf{r}$ satisfies $r_l/(\sum_{i=1}^M r_i+1)\le b_l$. Hence, the following Problem **2** has a larger feasible set than Problem **1**: (Problem **2**)

$$\bar{\Delta}^{\text{w-peak}}_{\text{opt},2}\triangleq\min_{r_l>0}\sum_{l=1}^{M}\frac{w_l e^{-r_l\frac{t_s}{\mathbb{E}[T]}}}{r_l}e^{\sum_{i=1}^M r_i\frac{t_s}{\mathbb{E}[T]}}\left(1+\sum_{i=1}^{M}r_i\right)+\sum_{l=1}^{M}w_l \tag{38}$$

$$\textbf{s.t. } r_l\le b_l\left(\sum_{i=1}^{M}r_i+1\right),\forall l, \tag{39}$$

where $\bar{\Delta}^{\text{w-peak}}_{\text{opt},2}$ is the optimal value of Problem **2**. The optimal objective value of Problem **2** is a lower bound of that of Problem **1**. We note that the constraint set corresponding to Problem **2** is convex. Thus, this relaxation converts the constraint set of Problem **1** to a convex one, and hence enables us to obtain a lower bound for the optimal value of Problem **1**, which is expressed as follows:

Lemma 4.3. *If $\sum_{i=1}^M b_i\ge 1$, then*

$$\bar{\Delta}^{w\text{-}peak}_{opt}\ge\bar{\Delta}^{w\text{-}peak}_{opt,2}\ge\sum_{i=1}^{M}\left[\frac{w_i}{\min\{b_i,\beta^\star\sqrt{w_i}\}}+w_i\right], \tag{40}$$

where $\beta^\star$ is the root of (20).

Proof. See our technical report [7]. □

Step 3: After the upper and lower bounds of $\bar{\Delta}^{\text{w-peak}}_{\text{opt}}$ were derived in Steps 1-2, we are ready to analysis their gap. By combining (36) and (40), the sub-optimality gap of the solution $\mathbf{r}^\star$ given by (18) - (20) is upper bounded by

$$\left|\bar{\Delta}^{\text{w-peak}}(\mathbf{r}^\star)-\bar{\Delta}^{\text{w-peak}}_{\text{opt}}\right|\le\sum_{i=1}^{M}\frac{w_i\left(e^{x^\star\frac{t_s}{\mathbb{E}[T]}(1+\frac{1}{x^\star})-1}\right)}{\min\{b_i,\beta^\star\sqrt{w_i}\}}, \tag{41}$$

where $x^\star$, $\beta^\star$ are defined in (19), (20). Next, we characterize the right-hand-side (RHS) of (41) by Taylor expansion. For simplicity, let $\epsilon=\frac{t_s}{\mathbb{E}[T]}$. Using the expression for $x^\star$ from (19), we have

$$x^\star\epsilon=-\frac{\epsilon}{2}+\sqrt{\frac{\epsilon^2}{4}+\epsilon}=\frac{\epsilon}{\frac{\epsilon}{2}+\sqrt{\frac{\epsilon^2}{4}+\epsilon}}=\sqrt{\epsilon}+o(\sqrt{\epsilon}). \tag{42}$$

Moreover,

$$x^\star = -\frac{1}{2} + \sqrt{\frac{1}{4} + \frac{1}{\epsilon}} = \frac{\frac{1}{\epsilon}}{\frac{1}{2} + \sqrt{\frac{1}{4} + \frac{1}{\epsilon}}} = \frac{1}{\sqrt{\epsilon}} + o\left(\frac{1}{\sqrt{\epsilon}}\right). \quad (43)$$

Substituting (42) and (43) in (41), we obtain

$$\begin{aligned}\left|\bar{\Delta}^{\text{w-peak}}(\mathbf{r}^\star) - \bar{\Delta}^{\text{w-peak}}_{\text{opt}}\right| &\leq \sum_{i=1}^{M} \frac{w_i[e^{\sqrt{\epsilon}+o(\sqrt{\epsilon})}(1+\sqrt{\epsilon}+o(\sqrt{\epsilon}))-1]}{\min\{b_i, \beta^\star\sqrt{w_i}\}} \\ &= \sum_{i=1}^{M} \frac{w_i[(1+\sqrt{\epsilon}+o(\sqrt{\epsilon}))(1+\sqrt{\epsilon}+o(\sqrt{\epsilon}))-1]}{\min\{b_i, \beta^\star\sqrt{w_i}\}} \\ &= 2\sqrt{\epsilon}\sum_{i=1}^{M} \frac{w_i}{\min\{b_i, \beta^\star\sqrt{w_i}\}} + o(\sqrt{\epsilon}), \end{aligned} \quad (44)$$

where the second inequality involves the use of Taylor expansion. This proves Theorem 3.1. Moreover, we can observe that the gap $\left|\bar{\Delta}^{\text{w-peak}}(\mathbf{r}^\star) - \bar{\Delta}^{\text{w-peak}}_{\text{opt}}\right|$ in the energy-adequate regime converges to zero at a speed of $O(\sqrt{\epsilon})$, as $\epsilon \to 0$. We also observe that both the upper and lower bounds (36), (40), converge to $\sum_{i=1}^{M}[(w_i/\min\{b_i, \beta^\star\sqrt{w_i}\}) + w_i]$ as $t_s/\mathbb{E}[T] \to 0$. Thus, this value is the asymptotic optimal value of Problem **1**. This proves Corollary 3.2.

5 NUMERICAL RESULTS

We use Matlab to evaluate the performance of our algorithm. We use "Age-optimal scheduler" to denote the sleep-wake scheduler with the sleep period paramters $r_l^\star$'s as in (18), which was shown to be near-optimal in Theorem 3.1 and Theorem 3.3. By "Throughput-optimal scheduler", we refer to the sleep-wake algorithm of [9] that is known to achieve the optimal trade-off between the throughput and energy consumption reduction. Moreover, we use "Fixed sleep-rate scheduler" to denote the sleep-wake scheduler in which the sleep period parameters r_l's are equal for all the sources, i.e., $r_l = k$ for all l, where the parameter k has been chosen so as to satisfy the energy constraints of Problem **1**. We also let $\bar{\Delta}^{\text{w-peak}}_{\text{un}}(\mathbf{r})$ denote the unnormalized total weighted average peak age in (11). Finally, we would like to mention that we do not compare the performance of our proposed algorithm with the CSMA algorithms of [25, 38] since the objective of these works was solely to minimize the age. Since they do not incorporate energy constraints, it is not fair to compare the performance of our algorithm with them.

Unless stated otherwise, our set up is as follows: The average transmission time is $\mathbb{E}[T] = 5$ ms. The weights w_l's attached to different sources are generated by sampling from a uniform distribution in the interval $[0, 10]$. The target energy efficiencies b_l's are randomly generated uniformly within the range $[0, 1]$.

We set the number of sources at $M = 10$. Figure 3 plots the total weighted average peak age $\bar{\Delta}^{\text{w-peak}}_{\text{un}}(\mathbf{r})$ in (11) as a function of the ratio $\frac{t_s}{\mathbb{E}[T]}$. The age-optimal scheduler is seen to outperform the throughput-optimal and Fixed sleep-rate schedulers. This implies that what minimizes the throughput does not necessarily minimize AoI and vice versa. Moreover, we observe that the total weighted average peak age of all schedulers increases as the sensing time increases. This is expected since an increase in the sensing time leads to an increase in the probability of packet collisions, which in turn deteriorates the age performance of these schedulers.

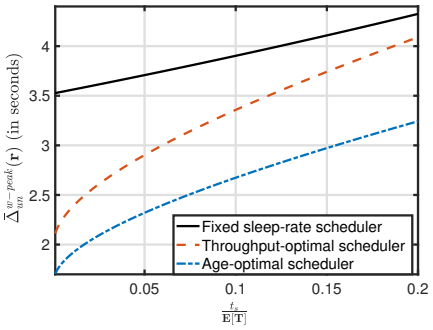

Figure 3: Total weighted average peak age $\bar{\Delta}^{\text{w-peak}}_{\text{un}}(\mathbf{r})$ in (11) versus the ratio $\frac{t_s}{\mathbb{E}[T]}$ for $M = 10$ sources.

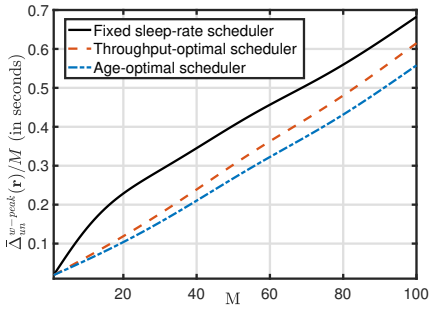

Figure 4: Total weighted average peak age $\bar{\Delta}^{\text{w-peak}}_{\text{un}}(\mathbf{r})$ in (11) versus the number of sources M, where $\bar{\Delta}^{\text{w-peak}}_{\text{un}}(\mathbf{r})$ has been normalized by M while plotting.

We then scale the number of sources M, and plot $\bar{\Delta}^{\text{w-peak}}_{\text{un}}(\mathbf{r})$ in (11) as a function of M in Figure 4. While plotting, we normalize the performance by the number of sources M. The sensing time t_s is fixed at $t_s = 40$ μs. The weights w_l's corresponding to different sources are randomly generated uniformly within the range $[0, 2]$. The age-optimal scheduler is shown to outperform other schedulers uniformly for all values of M. Moreover, as we can observe, the average peak age of the sources under age-optimal scheduler increases up to around 0.55 seconds only, while the number of sources rises from 1 to 100. This indicates the robustness of our algorithm to changes in the number of sources in a network.

In Figure 5, we fix the value of M at 100 sources and the target energy efficiencies at the same value for all the sources, i.e., $b_l = b$ for all l. We then vary the parameter b and plot the resulting performances. While plotting, we normalize the performance by the number of sources M. We exclude the simulation of the throughput-optimal scheduler for $b < 0.01$ since the sleeping period parameters that are proposed in [9] are not feasible for Problem **1** in energy-scarce regime, i.e., when $\sum_{i=1}^{M} b_i < 1$. The age-optimal scheduler outperforms the rest of the schedulers. Moreover, its performance is a decreasing function of b, and then settles at a constant value. This occurs because we observe from (18) that there exists a value

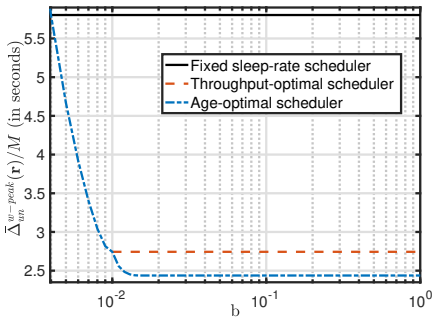

Figure 5: Total weighted average peak age $\bar{\Delta}_{\text{un}}^{\text{w-peak}}(\mathbf{r})$ in (11) versus the target energy efficiency b for $M = 100$ sources, where $\bar{\Delta}_{\text{un}}^{\text{w-peak}}(\mathbf{r})$ has been normalized by M while plotting.

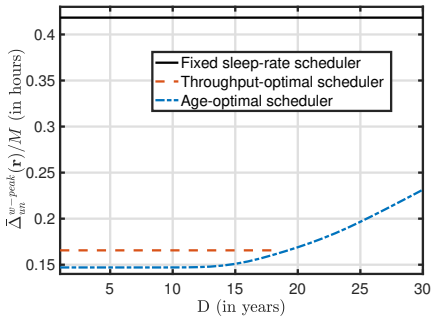

Figure 6: Total weighted average peak age $\bar{\Delta}_{\text{un}}^{\text{w-peak}}(\mathbf{r})$ in (11) versus the target lifetime D for a dense network with number of sources $M = 10^5$, where $\bar{\Delta}_{\text{un}}^{\text{w-peak}}(\mathbf{r})$ has been normalized by M while plotting. Since the throughput–optimal scheduler is infeasible for values of D greater than 18 years, we do not plot its performance for these values.

for b after which our proposed solution value, $\mathbf{r}^\star$, is a function solely of weights w_l's and $\beta^\star$, and not of b. Thus, the performance of the proposed scheduler saturates after this value of b.

We now show the effectiveness of the proposed scheduler when deployed in "dense networks" [21, 22]. Dense networks are characterized by a large number of sources connected to a single AP. We fix M at 10^5 sources, and take the target lifetimes of the sources to be equal, i.e., $D_l = D$ for all l. The weights w_l's corresponding to different sources are generated randomly by sampling from the uniform distribution in the range $[0, 2]$. We let the initial battery level $B_l = 8$ mAh for all l and the output voltage is 5 Volt. We also let the energy consumption in a transmission mode to be 24.75 mW for all sources. We vary the parameter D and plot the resulting performance in Figure 6. While plotting, we normalize the performance by the number of sources M. We exclude simulations for the throughput-optimal scheduler for values of D for which the scheduler is infeasible, i.e., its cumulative energy consumption exceeds the total allowable energy consumption. The age-optimal scheduler is seen to outperform the others. As observed in Figure 6, under the age-optimal scheduler, sources can be active for up to

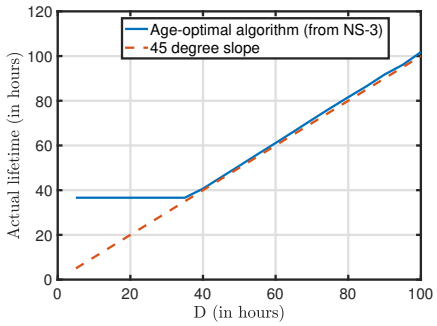

Figure 7: The average actual lifetime versus the target lifetime D.

25 years, while simultaneously achieving a decent average peak age of around .2 hour, i.e., 12 minutes. This makes it apt for dense networks, where it is crucial that the sources are necessarily active for many years.

5.1 NS-3 Simulation

We use NS-3 [26] to investigate the effect of our assumptions on the performance of the age-optimal scheduler in a more practical situation. We simulate the Age-optimal scheduler by using IEEE 802.11b by disabling the RTS-CTS and modifying the back-off times to be exponentially distributed in the MAC layer. Our simulation results are averaged over 5 system realizations. The UDP saturation conditions are satisfied such that all source nodes always have a packet to send.

Our simulation consists of a WiFi network with 1 AP and 3 associated source nodes in a field of size 50m × 50m. We set the sensing threshold to -100 dBm which covers a range of 110m. Thus, all sources can hear each other. We set the initial battery level of all source to be 60 mAh, where the output voltage is 5 Volt. For each source, the power consumption in the transmission mode is 24.75 mW, and the power consumption in the sleep mode is 15 μW. Moreover, all weights are set to unity, i.e., $w_l = 1$ for all l.

Figure 7 plots the average actual lifetime of the sources versus the target lifetime, where we take the target lifetimes of all sources to be equal, i.e., $D_l = D$ for all l. As we can observe, the actual lifetime of the age-optimal scheduler always achieves the target lifetime. This suggests that our assumptions (i.e., (i) omitting the power dissipation in the sleep mode and in the sensing times, (ii) the average transmission times and collision times are equal to each other) do not affect the performance of the algorithm which reaches its target lifetime.

Figure 8 plots the total weighted average peak age versus the target lifetime, where again we take the target lifetimes of all sources to be equal, i.e., $D_l = D$ for all l. The age-optimal scheduler (theoretical) curve is obtained using (11), while the age-optimal scheduler (from NS-3) curve is obtained using the NS-3 simulator. As we can observe, the difference between the plotted curves does not exceed 2% of the age-optimal scheduler (theoretical) performance. This emphasizes the negligible impact of our assumptions on the performance of our proposed algorithm.

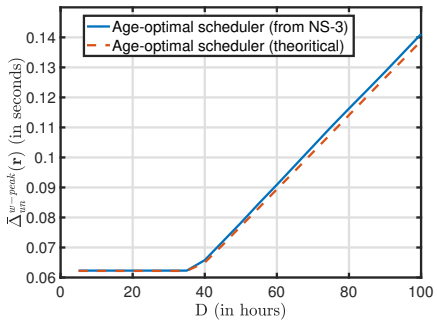

Figure 8: Total weighted average peak age $\bar{\Delta}_{\mathbf{un}}^{\mathbf{w\text{-}peak}}(\mathbf{r})$ versus the target lifetime D.

6 CONCLUSIONS

We designed an efficient sleep-wake mechanism for wireless networks that attains the optimal trade-off between minimizing the AoI and energy consumption. Since the associated optimization problem is non-convex, in general we could not hope to solve it for all values of the system parameters. However, in the regime when the carrier sensing time t_s is negligible as compared to the average transmission time $\mathbb{E}[T]$, we were able to provide a near-optimal solution. Moreover, the proposed solution is on a simple form that allowed us to design a simple-to-implement algorithm to obtain its value. Finally, we showed that, in the energy-adequate regime, the performance of our proposed algorithm is asymptotically no worse than that of the optimal synchronized scheduler, as $t_s/\mathbb{E}[T] \to 0$.

ACKNOWLEDGMENTS

The authors appreciate Jiayu Pan and Shaoyi Li for their great efforts in obtaining the ns-3 simulation results.

This work has been supported in part by NSF grants 1618520, 1901057, 1719371, and CCF-1813050, by ONR grant N00014-17-1-2417, N00014-17-1-2417, and by the IITP grant (MSIT), (2017-0-00692), Transport-aware Streaming Technique Enabling Ultra Low-Latency AR/VR Services.

REFERENCES

[1] A. M. Bedewy, Y. Sun, S. Kompella, and N. B. Shroff. Age-optimal Sampling and Transmission Scheduling in Multi-Source Systems. In *Proc. MobiHoc.* 121–130.
[2] A. M. Bedewy, Y. Sun, S. Kompella, and N. B. Shroff. submitted to *IEEE Trans. Inf. Theory*, 2020. Optimal Sampling and Scheduling for Timely Status Updates in Multi-source Networks. (submitted to *IEEE Trans. Inf. Theory*, 2020). https://arxiv.org/abs/2001.09863.
[3] A. M. Bedewy, Y. Sun, and N. B. Shroff. 2016. Optimizing data freshness, throughput, and delay in multi-server information-update systems. In *Proc. IEEE ISIT.* 2569–2573.
[4] A. M. Bedewy, Y. Sun, and N. B. Shroff. 2017. Age-optimal information updates in multihop networks. In *Proc. IEEE ISIT.* 576–580.
[5] A. M. Bedewy, Y. Sun, and N. B. Shroff. 2019. The age of information in multihop networks. *IEEE/ACM Trans. Netw.* 27, 3 (2019), 1248–1257.
[6] A. M. Bedewy, Y. Sun, and N. B. Shroff. 2019. Minimizing the age of information through queues. *IEEE Trans. Inf. Theory* 65, 8 (2019), 5215–5232.
[7] A. M. Bedewy, Y. Sun, R. Singh, and N. B. Shroff. 2019. Optimizing Information Freshness using Low-Power Status Updates via Sleep-Wake Scheduling. *arXiv preprint arXiv:1910.00205* (2019).
[8] G. Bianchi. 2000. Performance analysis of the IEEE 802.11 distributed coordination function. *IEEE J. Sel. Areas Commun.* 18, 3 (2000), 535–547.
[9] S. Chen, T. Bansal, Y. Sun, P. Sinha, and N. B. Shroff. 2013. Life-Add: Lifetime Adjustable design for WiFi networks with heterogeneous energy supplies. In *Proc. WiOpt.* 508–515.
[10] M. Costa, M. Codreanu, and A. Ephremides. 2016. On the Age of Information in Status Update Systems With Packet Management. *IEEE Trans. Inf. Theory* 62, 4 (2016), 1897–1910.
[11] A. El-Hoiydi. 2002. Spatial TDMA and CSMA with preamble sampling for low power ad hoc wireless sensor networks. In *Proc. IEEE Int. Symp. Comput. Commun. (ISCC).* 685–692.
[12] X. Guo, R. Singh, P. R. Kumar, and Z. Niu. 2018. A Risk-Sensitive Approach for Packet Inter-Delivery Time Optimization in Networked Cyber-Physical Systems. *IEEE/ACM Trans. Netw.* 26, 4 (2018), 1976–1989.
[13] Q. He, D. Yuan, and A. Ephremides. 2017. Optimal link scheduling for age minimization in wireless systems. *IEEE Trans. Inf. Theory* 64, 7 (2017), 5381–5394.
[14] P. Hsieh and I. Hou. 2018. A decentralized medium access protocol for real-time wireless ad hoc networks with unreliable transmissions. In *IEEE 38th International Conference on Distributed Computing Systems (ICDCS).* 972–982.
[15] Y. Hsu, E. Modiano, and L. Duan. 2019. Scheduling algorithms for minimizing age of information in wireless broadcast networks with random arrivals. *IEEE Transactions on Mobile Computing* (2019).
[16] L. Jiang and J. Walrand. 2010. A distributed CSMA algorithm for throughput and utility maximization in wireless networks. *IEEE/ACM Trans. Netw.* 18, 3 (2010), 960–972.
[17] Zhiyuan Jiang, Bhaskar Krishnamachari, Xi Zheng, Sheng Zhou, and Zhisheng Niu. 2018. Timely status update in massive IoT systems: Decentralized scheduling for wireless uplinks. *arXiv preprint arXiv:1801.03975* (2018).
[18] I. Kadota, A. Sinha, and E. Modiano. 2018. Optimizing age of information in wireless networks with throughput constraints. In *Proc. INFOCOM.* 1844–1852.
[19] I. Kadota, A. Sinha, E. Uysal-Biyikoglu, R. Singh, and E. Modiano. 2018. Scheduling Policies for Minimizing Age of Information in Broadcast Wireless Networks. *IEEE/ACM Trans. Netw.* 26, 6 (2018), 2637–2650.
[20] S. Kaul, R. D. Yates, and M. Gruteser. 2012. Real-time status: How often should one update?. In *Proc. IEEE INFOCOM.* 2731–2735.
[21] S. S. Kowshik, K. Andreev, A. Frolov, and Y. Polyanskiy. 2019. Energy efficient coded random access for the wireless uplink. *arXiv preprint arXiv:1907.09448* (2019).
[22] S. S. Kowshik and Y. Polyanskiy. 2019. Fundamental limits of many-user MAC with finite payloads and fading. *arXiv preprint arXiv:1901.06732* (2019).
[23] R. Li, A. Eryilmaz, and B. Li. 2013. Throughput-optimal wireless scheduling with regulated inter-service times. In *Proc. IEEE INFOCOM.* 2616–2624.
[24] C. Lu, A. Saifullah, B. Li, M. Sha, H. Gonzalez, D. Gunatilaka, C. Wu, L. Nie, and Y. Chen. 2016. Real-Time Wireless Sensor-Actuator Networks for Industrial Cyber-Physical Systems. *Proc. IEEE* 104, 5 (2016), 1013–1024.
[25] A. Maatouk, M. Assaad, and A. Ephremides. 2019. Minimizing The Age of Information in a CSMA Environment. *arXiv preprint arXiv:1901.00481* (2019).
[26] NS-3. . https://www.nsnam.org/.
[27] K. F. Ramadan, M. I. Dessouky, M. Abd-Elnaby, and F. E. A. El-Samie. 2016. Energy-efficient dual-layer MAC protocol with adaptive layer duration for WSNs. In *11th International Conference on Computer Engineering Systems (ICCES).* 47–52.
[28] A. N. Shiryaev. 1978. *Optimal stopping rules.* New York: Springer-Verlag.
[29] Y. Sun and B. Cyr. 2019. Sampling for data freshness optimization: Non-linear age functions. *Journal of Communications and Networks* 21, 3 (2019), 204–219.
[30] Y. Sun, I. Kadota, R. Talak, and E. Modiano. 2019. Age of Information: A New Metric for Information Freshness. *Synthesis Lectures on Communication Networks* 12, 2 (2019), 1–224.
[31] Y. Sun, E. Uysal-Biyikoglu, and S. Kompella. 2018. Age-optimal updates of multiple information flows. In *IEEE INFOCOM - the 1st Workshop on the Age of Information (AoI Workshop).* 136–141.
[32] Y. Sun, E. Uysal-Biyikoglu, R. D. Yates, C. E. Koksal, and N. B. Shroff. 2017. Update or Wait: How to Keep Your Data Fresh. *IEEE Trans. Inf. Theory* 63, 11 (2017), 7492–7508.
[33] R. Talak, S. Karaman, and E. Modiano. 2018. Distributed scheduling algorithms for optimizing information freshness in wireless networks. In *Proc. IEEE SPAWC.* 1–5.
[34] R. Talak, S. Karaman, and E. Modiano. 2018. Optimizing information freshness in wireless networks under general interference constraints. In *Proc. MobiHoc.* 61–70.
[35] N. F. Timmons and W. G. Scanlon. 2004. Analysis of the performance of IEEE 802.15. 4 for medical sensor body area networking. In *First Annual IEEE Communications Society Conference on Sensor and Ad Hoc Communications and Networks. IEEE SECON 2004.* 16–24.
[36] ASH transceiver TR1000 data sheet, RF Monolithic Inc. .
[37] A. Wald. 1973. *Sequential analysis.* New York: Courier Corporation.
[38] M. Wang and Y. Dong. 2019. Broadcast Age of Information in CSMA/CA Based Wireless Networks. *arXiv preprint arXiv:1904.03477* (2019).
[39] R. D. Yates and S. K. Kaul. 2017. Status updates over unreliable multiaccess channels. In *Proc. IEEE ISIT.* 331–335.
[40] R. D. Yates and S. K. Kaul. 2018. The age of information: Real-time status updating by multiple sources. *IEEE Trans. Inf. Theory* 65, 3 (2018), 1807–1827.
[41] S. Yun, Y. Yi, J. Shin, et al. 2012. Optimal CSMA: a survey. In *Proc. ICCS.* 199–204.